

ChemComm

Accepted Manuscript



This article can be cited before page numbers have been issued, to do this please use: M. Zgorzelak, J. Grajewski, J. Gawronski and M. Kwit, *Chem. Commun.*, 2019, DOI: 10.1039/C8CC10184A.



This is an Accepted Manuscript, which has been through the Royal Society of Chemistry peer review process and has been accepted for publication.

Accepted Manuscripts are published online shortly after acceptance, before technical editing, formatting and proof reading. Using this free service, authors can make their results available to the community, in citable form, before we publish the edited article. We will replace this Accepted Manuscript with the edited and formatted Advance Article as soon as it is available.

You can find more information about Accepted Manuscripts in the [author guidelines](#).

Please note that technical editing may introduce minor changes to the text and/or graphics, which may alter content. The journal's standard [Terms & Conditions](#) and the ethical guidelines, outlined in our [author and reviewer resource centre](#), still apply. In no event shall the Royal Society of Chemistry be held responsible for any errors or omissions in this Accepted Manuscript or any consequences arising from the use of any information it contains.

Journal Name

COMMUNICATION

Solvent-assisted synthesis of shape-persistent chiral polyaza gigantocycle characterized by a very large internal cavity and extraordinarily high amplitude of the ECD exciton couplet

Mikołaj Zgorzelak,^{*a} Jakub Grajewski,^a Jacek Gawroński,^a and Marcin Kwit^{*a,b}Received 00th January 20xx,
Accepted 00th January 20xx

DOI: 10.1039/x0xx00000x

www.rsc.org/

A giant, chiral square-shaped octaimine macrocycle has been obtained in a controlled manner from readily available and inexpensive substrates: 9,10-diphenylanthracene-based dialdehyde and *trans*-1,2-diaminocyclohexane. Reduction of the polyimine led to chiral octaimine characterized by a very large internal hydrophobic cavity.

Shape-persistent macrocycles have become one of the most important organic compounds useful in many aspects of chemistry among the macrocyclic structures known so far. These compounds may act as supramolecular building blocks forming various architectures in the solid state and in solution, scaffolds for artificial receptors and porous solids.¹ Generally, the shape-persistent macrocycles have a regular structure characterized by alternatively repeated units, which in principle, should simplify synthesis. However, due to the need to achieve a high level of substrate pre-organization, controlled synthesis of shape-persistent macrocycles larger than 50-membered (*gigantocycles*), represents still a challenging task.^{2,3}

Based on the Dynamic Covalent Chemistry concept thermodynamically controlled and reversible formation of the imine C=N double bonds gives a chance for obtaining cyclic compounds, if energy gain associated with the formation of cyclic products disfavors formation of acyclic oligomers.⁴ Since our pioneering work, the interest in template-free synthesis and subsequent applications of chiral polyimine and polyamine macrocycles is still increasing.⁵⁻⁸ Success of cycloimination reactions relies primarily on the proper choice of substrates that should be structurally predisposed to form chiral strain-free cyclic structures. So far, it has been an axiom to say that the combination of optically pure *trans*-1,2-diaminocyclohexane

(DACH, **1**) and linear 1,4-dialdehyde leads to a highly symmetrical product with [3+3] stoichiometry and a triangle structure (*trianglimine*). It is believed that this particular cycloimination reactions proceed smoothly, irrespective to the substitution pattern in the 1,4-dialdehyde skeleton, solvent polarity and concentration of the substrates.^{8,9}

While the terephthalaldehyde and 4,4'-diformylidiphenyl derivatives are the most common substrates, anthracene-based derivatives have been used very rarely in cycloimination reactions. Due to a poor solubility in organic solvents, difficulties in synthesis and in proper characterizations, there are only two examples of chiral [3+3] triangular polyimine macrocycles containing anthracene moieties known to date.¹⁰ This remains in contrast to a number of macrocyclic structures built on the basis on 9,10-anthracene and 9,10-diphenylanthracene units. Being highly fluorescent, the latest derivatives and their heteroatom analogs are frequently used for construction of light-emitting materials.¹¹ The characteristic feature of 9,10-diphenylanthracene is the almost perpendicular orientation of the anthracene and phenyl units associated with hindered rotation around C_{Ar}-C_{Ar} bonds.¹²

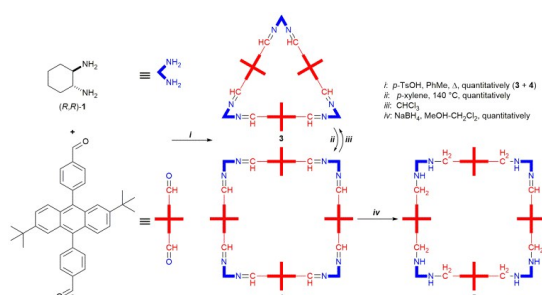
We reasoned that an addition of bulky, hydrophobic *tert*-butyl groups to the 9,10-diphenylanthracene skeleton would make the parent aldehyde and the resulting macrocycle more soluble in organic solvents. On the other hand, the presence of bulky groups attached to the anthracene significantly increases steric strains and may completely prevent macrocyclization. Thus, we expanded our study into chiral polyimine 9,10-diphenylanthracene derivatives to demonstrate the influence of the aldehyde structure and/or reaction conditions on the structure of the product(s). Meanwhile, we anticipated that the newly synthesized chiral macrocycles, containing very complex chromophoric systems, might constitute interesting objects for the study with the use of the electronic circular dichroism (ECD) spectroscopy. Interactions between electric dipole transition moments (EDTMs) polarized within aromatic chromophores should lead to strong exciton Cotton effects (CEs), allowing the

^a Department of Chemistry, Adam Mickiewicz University, Umultowska 89B, 61 614 Poznań, Poland; e-mail: mikolaj.zgorzelak@amu.edu.pl or marcin.kwit@amu.edu.pl

^b Centre for Advanced Technologies, Adam Mickiewicz University, Umultowska 89C, 61 614 Poznań, Poland.

† Electronic Supplementary Information (ESI) available: [enlarged versions of Scheme 1 and Figures, experimental procedures, calculation details, copies of ¹H and ¹³C NMR spectra]. See DOI: 10.1039/x0xx00000x

interpretation of the ECD spectra in terms of exciton chirality rule.^{9,13}



Scheme 1. Synthesis of macrocycles [3+3]-**3**, [4+4]-**4** and [4+4]-**5** (see ESI for enlarged version).

The synthesis of a new *tert*-butyl-substituted dialdehyde **2** was achieved by a three-step sequence of reactions from inexpensive reagents and without a column chromatography (see ESI). The initial attempts to obtain macrocycle from (*R,R*)-**1** and **2** have failed. In conditions typical of cycloimination reactions (chloroform, RT, 24 h),⁸ we did not observe the full substrate conversion and the mass spectrum indicated the presence of many different products, mainly open-chain, in the reaction mixture. However, the reaction carried out in a boiling toluene and in the presence of catalytic amounts of *p*-toluenesulfonic acid, unexpectedly, provided the mixture of two products. The conversion of substrates was complete and in no case, did we observe the formation of linear oligomers. Mass spectrometry indicated that the mixture consisted of [3+3]-**3** and [4+4]-**4** macrocycles. The **3:4** ratio was approximately equimolar as estimated on the basis on integration of the CHN imine signals appeared at $\delta = 8.51$ and 8.27 in diagnostic region of the ¹H NMR spectrum (Figure 1a). The heating of the suspension of **3** and **4** in *p*-xylene at boiling point (140 °C) led to a transparent, deep-yellow colored solution, which has become turbid and yellow-green-colored after cooling to temperature below 100 °C. At this point, the complete conversion of the smaller 66-membered macrocycle **3** into its larger 88-membered counterpart **4** was observed (see Figure 1b). High boiling point of the solvent is not a sufficient condition and none of the other organic solvents caused expansion of the macro ring. It is worth noting that macrocycle **4** can be obtained as the main product if the condensation reactions are carried out immediately in *p*-xylene. The remaining xylene isomers as well as other aromatic solvents in the above reaction conditions always lead to a mixture of products (see ESI).

The square-shaped macrocycle **4** is isolated as the complex with two molecules of *p*-xylene. The solvent can be partially removed from the solid material by prolonged drying under very high vacuum and at elevated temperature. *p*-Xylene functions as a template to facilitate preorganization of the sub-units which form the macrocycle. This type of solvent-assisted transformation has never been reported for chiral polyimines. Although the detailed explanation of such phenomenon is not known at the moment, minimizing the dipole moment in the tetrameric structure together with CH \cdots π and $\pi\cdots\pi$ stacking interactions between the solvent and the macrocycle formed

can be of particular importance. The macrocycle **4** is stable in the solid state. However, in solution, **4** undergoes step-wise decomposition, which is slowed down in the presence of an excess of triethylamine.

The ¹H NMR recorded at specific time intervals for the macrocycle **4**, carried out in dry, pure CDCl₃ (Figure 2a,b), gave an insight into the course of the equilibration process. A contraction of macrocycle **4** into **3** started immediately upon dissolution, ran through an open-chain intermediate product and within 5 hours, the mixture reached equilibrium. The reaction equilibrium constant has been calculated as 1.1.

At a reduced temperature, we observed broadening of the respective aromatic ¹H NMR signals of imine **4**. Unfortunately, below -40 °C the macrocycle precipitated from chloroform solution, prevented further study (see ESI). A subsequent reduction of **4**, by simply treatment with sodium borohydride in methanol-dichloromethane solution, led to chemically stable octaamine **5**. The characteristic for neutral **5**, ArCH₂N benzyl protons, appeared as two doublets at $\delta = 4.14$ and 3.90 , shifted downfield upon protonation of the amine by trifluoroacetic acid ($\delta = 4.65$ and 4.43 , Figures 1c,d). The number of diagnostic signals, which appeared in ¹H and ¹³C NMR spectra of **4** and **5**, suggests their high symmetry.

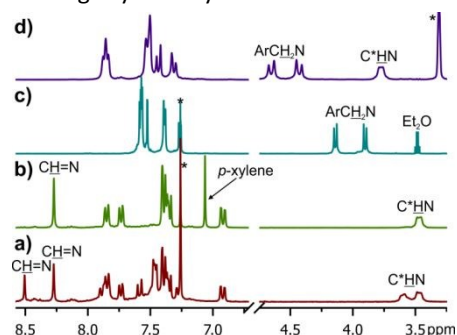


Figure 1. Diagnostic parts of ¹H NMR spectra of: a) crude mixture of **3** and **4** [CDCl₃]; b) pure **4**×2(*p*-xylene) [CDCl₃]; c) octaamine **5** [CDCl₃] and d) protonated octaamine **5**×8H⁺ [CD₃OD+TFA]. Asterisks indicate trace solvent peaks.

The shape of ¹H NMR spectrum of **5**×8H⁺ has changed upon increasing the temperature of measurement (Figure 2c). The higher temperatures increased conformational freedom of the aromatic linkers and allowed anthracenes to rotate around C_{Ar}-C_{Ar} carbon bonds. Phenyl rotation barrier in 9-phenylanthracene, estimated by Nikitin and co-workers, is ca. 21 kcal mol⁻¹.¹² However, the macrocycle **5**×8H⁺ represents much more complex system due to a double substitution of each anthracene and possibility of gearing of anthracene fragments. The difficulty in obtaining suitable crystals prevents the use of X-ray diffraction for structure elucidations. Hence, the use of experimental ECD measurements supported by theoretical calculations of structure and spectra at the DFT¹⁵ level seems to be the method of choice for structural studies of these macrocycles. The calculated low-energy structures of **3**, **4**, **5** and **5**×8H⁺ are shown in Figure 3. As expected, the characteristic feature for all macrocycles under study is a non-planar orientation of anthracene and phenylene units associated with hindered rotation around aryl-aryl single bonds. Therefore, at normal conditions the aromatic linker can only rotate around

the C_{Ar} -CHN single bonds. The triangular imine **3** is characterized by highly congested structure, in which *tert*-butyl groups are situated at close proximity. Expansion of the macrocyclic ring might release the sterical overcrowding at the expense of the loss of the linear structure of the linkers. The calculated low-energy structure of **4** can be very roughly treated as the equivalent of cyclobutane – two apexes are above and the remaining two are positioned below the mean macrocycle plane. Similarly, the *tert*-butyl substituted anthracene moieties are alternatively positioned below and above the mean macrocycle plane. In two facing linkers, the phenylene rings remain perpendicular to the anthracene plane, whereas in the remaining two, are distorted from perpendicularity. The aromatic linkers close the cavity and do not allow inclusion inside the macrocycle.

The comparison of calculated total energies led to the conclusion that the smaller one, **3**, is more energetically preferable than its larger counterpart **4** is. The energy cost associated with ring expansion is around 16 kcal mol⁻¹. Therefore, the octaimine **4** is a rather metastable compound that persists in the solid state.

In addition to the increase in chemical stability, reduction of the imine bonds changes the macrocycle structure. Due to the possibility of the configuration inversion at the nitrogen atoms and unhindered rotation around (C_{Ar})CH₂-N bonds, the linkers may adopt conformation in which the bulky elements are far away from each other. On the other hand, the formation of NH...N hydrogen bonding is recognized as a key factor that stabilize structure of triaminines.¹⁶ From the two stable low-energy structures of **5**, found by calculations, the C_4 -symmetrical one is characterized by the presence of four intramolecular NH...N hydrogen bonds, which forces the bowl-shaped conformation (see Figure S2, ESI). However, the repulsion between *tert*-butyl groups raises the energy of the molecule by 13 kcal mol⁻¹, as computational conformational analysis indicates, therefore, excluding this conformer from considerations. On the other hand, the lowest energy conformer of **5** and $5 \times 8H^+$ are both characterized by the high D_4 symmetry and similar structure. In both **5** and $5 \times 8H^+$, the anthracene units are perpendicular, whereas phenylene groups are positioned, alternatively, above and below the mean macrocycle plane. Such conformation of aromatic linkers opens the hydrophobic internal cavity of the macrocycle. The distance between the middle points of anthracene units is 21.36 Å that corresponds to radius of a circle inscribed in a square of 10.68 Å. So far, macrocycle **5** represents the first DACH-based and shape-persistent chiral polyamine, characterized by such a large internal cavity. The ECD spectrum of octaimine **4** (Figure 4a) is dominated by the strong exciton negative couplet of amplitude $A = -1380$ that appeared at around 270 nm and corresponding to the UV absorption maximum of $\epsilon = 480000$. Such a high-intense exciton couplet has never been reported for chiral polyimine compounds. Reduction of imine bonds and related change in structure and electron properties of the chromophore, significantly affected the ECD and UV spectra of **5**. Although the most intense UV absorption band still appears at around 270 nm ($\epsilon = 383100$), the exciton couplet associated

with this band is characterized by much lower magnitude ($A = 267$) and by inverted sign. Protonation of **5** did not alter significantly the observed absorption bands and CEs, confirming by this way similar structure of **5** and $5 \times 8H^+$ species. The macrocycle **4** contains very complex chromophoric systems, each of them is made of three sub-units. Due to the almost perpendicular orientation of phenylene and anthracene rings in linkers, there is no possibility for electron delocalization within the chromophore. The aromatic linker in **4** consists of an anthracene chromophore flanked by two ArCH=N (imine) chromophores each of which gives an individual contribution to the overall ECD spectrum.

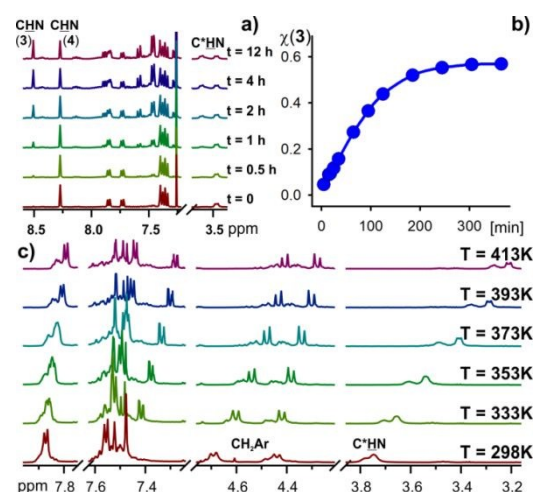


Figure 2. a) Traces of ¹H NMR spectra [CDCl₃] measured for **4** at certain time intervals. b) Contraction of **4** measured as the increase of the mole fraction of **3** ($\chi(3)$). c) Variable temperature ¹H NMR spectra of $5 \times 8H^+$ [DMSO-*d*₆ + TFA].

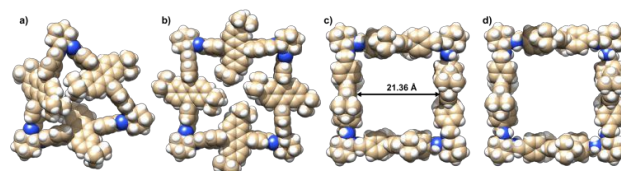


Figure 3. Low-energy structures of a) imine **3**; b) imine **4**; c) amine **5** and d) octaprotonated amine $5 \times 8H^+$ calculated at the B3LYP/6-311G(d,p) level.

Using model compound **6** and Coulomb-attenuating method (see ESI for details),¹⁵ the polarizations of the main electronic transitions responsible for exciton couplets have been determined. The calculated lowest-energy π - π^* (HOMO-LUMO) electronic transition is polarized along the main axis of the molecule. Due to the long distance between the electric dipole transition moments, these interactions are not resulted in strong exciton-type CEs in experimental spectrum of **4**. The transitions no 2 and 4 involve ArCH=N orbitals. The EDTM's associate with these transitions is distorted from the main axis of **6**. The transition no 3, involving anthracene orbitals, is characterized by the highest oscillator strength and polarized along the long axis of anthracene (Figures 4c). However, the generated exciton couplets are dependent on spatial orientations of chromophores in **4** and they are alternately positive and negative. Therefore, the imine-imine interactions are mainly responsible for observed experimentally in ECD spectrum of **4** strong negative couplet. The interactions between the adjacent imine and anthracene chromophores are less important (see Table S1, ESI).

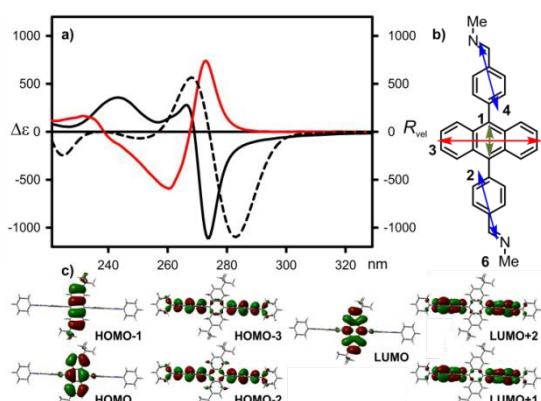


Figure 4. a) Experimental (solid lines) of **4** (black line) and **5** (red line) and calculated at the ZINDO level (dashed black line) ECD spectrum of **4**. Due to the low intensity, the ECD spectrum of **5** was multiplied by the factor of 5. Wavelengths were not corrected. b) Estimated polarizations and c) orbitals involved in the main electronic transitions calculated for model compound **6**.

The results of the empirical analysis remain in agreement with the experiment. The empirical analysis was supported by semi-quantitative calculations of ECD spectra of interacting chromophoric fragments.¹⁷ The contribution from all imine-imine interactions is almost 5 times as large as that from anthracene-anthracene interactions (see ESI for details). Furthermore, these empirical and semi-quantitative analyses were confirmed by the calculations of ECD spectrum of **4**. Even for a relatively low level of theory, the compatibility of experimental and theoretical data remains in good agreement (Figure 3a). The same theoretical analysis carried out for **5** provided results that are in agreement with experimental ECD data, therefore confirming postulated structure of **5** (see ESI).

We have presented here synthesis and structural studies on chiral gigantocycles, characterized by the unusual square-shape. The synthesis of this type of compounds is in contradiction with the generally accepted view on the [3+3] selectivity of the condensation reaction between (*R,R*)-**1** and linear aldehydes. The solvent controlled synthesis of such large systems gives a chance for their later use. The reduced macrocycle **5** and its protonated counterpart represent polyimine-derived rings of the highest value of internal cavity known so far. Preliminary experiments indicated these macrocycles as good precursors of new materials. Although, the initial attempts to obtain porous material from **4** were unsuccessful and the estimated value of the Brunauer-Emmett-Teller surface area (S_{BET}) was below $5 \text{ m}^2 \text{ g}^{-1}$, the open structure of **5** significantly increased measured S_{BET} value up to $149 \text{ m}^2 \text{ g}^{-1}$. Due to the mismatch of the host and guest molecules, **5** cannot act as a receptor for C_{60} or C_{70} fullerenes. A very rough estimation indicates that only fullerenes with a size between C_{96} and C_{240} give a chance for effective binding to the host molecule. Further studies are in progress in our laboratory.

Conflicts of interest

There are no conflicts to declare.

Notes and references

- W. Zhang and J. S. Moore, *Angew. Chem. Int. Ed.*, 2006, **45**, 4416 and references therein. DOI: 10.1039/C8CC10184A
- a) V. Martí-Centelles, M. D. Pandey, M. I. Burguete and S. V. Luis, *Chem. Rev.*, 2015, **115**, 8736; b) L. A. Wessjohann, D. G. Rivera and O. E. Vercillo, *Chem. Rev.*, 2009, **109**, 796; c) Y. Jin, C. Yu, R. J. Denman and W. Zhang, *Chem. Soc. Rev.*, 2013, **42**, 6634.
- a) V. Prautzsch, S. Ibach and F. Vögtle, *J. Inclusion Phen.*, 1999, **33**, 427; b) M. R. Shah, S. Duda, B. Müller, A. Godt and A. Malik, *J. Am. Chem. Soc.*, 2003, **125**, 5408.
- a) S. J. Rowan, S. J. Cantrill, G. R. L. Cousins, J. K. M. Sanders and J. F. Stoddart, *Angew. Chem. Int. Ed.*, 2002, **41**, 898; b) P. T. Corbett, J. Leclaire, L. Vial, K. R. West, J.-L. Wietor, J. K. M. Sanders and S. Otto, *Chem. Rev.*, 2006, **106**, 3652.
- J. Gawroński, H. Kołbon, M. Kwit and A. Katrusiak, *J. Org. Chem.*, 2000, **65**, 5768.
- a) M. E. Belowich and J. F. Stoddart, *Chem. Soc. Rev.*, 2012, **41**, 2003; b) N. E. Borisova, M. D. Reshetova and Y. A. Ustynyuk, *Chem. Rev.*, 2007, **107**, 46; c) S. Srimurugan, P. Suresh, B. Babu and H. N. Pati, *Mini-Rev. Org. Chem.*, 2008, **5**, 228.
- J. Gawroński, M. Kwit and U. Rychlewska, in *Comprehensive Supramolecular Chemistry II*, (Eds.: J. L. Atwood, G. W. Gokel, L. J. Barbour) Oxford: Elsevier, 2017, vol. 3, pp. 267–291, and references therein.
- M. Kwit, J. Grajewski, P. Skowronek, M. Zgorzelak and J. Gawroński, *Chem. Rec.*, DOI: 10.1002/tcr.201800052.
- N. Prusinowska, M. Bardziński, A. Janiak, P. Skowronek and M. Kwit, *Chem. Asian J.*, 2018, **13**, 2691.
- a) M. Kwit, P. Skowronek, H. Kołbon and J. Gawroński, *Chirality*, 2005, **17**, S93; b) N. Kuhnert, C. Patel and F. Jami, *Tetrahedron Lett.*, 2005, **46**, 7575.
- see for example: a) R. Yamakado, S. Matsuoka, M. Suzuki, D. Takeuchi, H. Masu, I. Azumaya and K. Takagi, *RSC Adv.*, 2014, **4**, 6752; b) S. S. Babu, M. J. Hollamby, J. Aimi, H. Ozawa, A. Saeki, S. Seki, K. Kobayashi, K. Hagiwara, M. Yoshizawa, H. Möhwald and T. Nakanishi, *Nat. Commun.*, 2013, **4**, 1969; c) Y. Fujiwara, R. Ozawa, D. Onuma, K. Suzuki, K. Yoza and K. Kobayashi, *J. Org. Chem.*, 2013, **78**, 2206; d) K. Hagiwara, Y. Sei, M. Akita and M. Yoshizawa, *Chem. Commun.*, 2012, **48**, 7678; e) J.-L. Liu, Z.-L. Tang, J.-Q. Zhang, Y.-Q. Chai, Y. Zhuo and R. Yuan, *Anal. Chem.* 2018, **90**, 5298; f) K. Yazaki, L. Catti and M. Yoshizawa, *Chem. Commun.*, 2018, **54**, 3195.
- K. Nikitin, H. Müller-Bunz, Y. Ortin, J. Muldoon and M. J. McGlinchey, *Org. Lett.*, 2011, **13**, 256.
- N. Harada, K. Nakanishi and N. Berova, in *Comprehensive Chiroptical Spectroscopy* (Eds N. Berova, P. L. Polavarapu, K. Nakanishi, R. W. Woody) Hoboken: Wiley, 2012.
- Previously, the solvent effects in multicomponent cage syntheses have been studied, see for example: a) S. Mecozzi and J. Rebek, *Chem. Eur. J.*, 1998, **4**, 1016; b) S. Lahiri, J. L. Thompson and J. S. Moore, *J. Am. Chem. Soc.*, 2000, **122**, 11315; c) X. Liu and R. Warmuth, *J. Am. Chem. Soc.*, 2006, **128**, 14120.
- Gaussian 09, Revision D.01, Gaussian, Inc., Wallingford CT, 2009. All calculations were performed at Poznan Supercomputing and Networking Centre.
- J. Gawronski, K. Gawronska, J. Grajewski, M. Kwit, A. Plutecka and U. Rychlewska, *Chem. Eur. J.* 2006, **12**, 1807.
- This procedure has been successfully used by us for interpretation of complex ECD spectra of multichromophoric systems, see for example: a) M. Kwit, J. Gawronski, D. R. Boyd, N. D. Sharma and M. Kaik, *Org. Biomol. Chem.*, 2010, **8**, 5635; b) N. Prusinowska, W. Bendzińska-Berus, J. Szymkowiak, B. Warzajtis, J. Gajewy, M. Jelecki, U. Rychlewska and M. Kwit, *RSC Adv.*, 2015, **5**, 83448.